A biological dipole variability in the Indian Ocean

Kyung Min Noh[1], Jong-Seong Kug[1], Gayan Pathirana[1], Dong-Geon Lee[1], and Huiji Lee[1]

[1]Affiliation not available

November 14, 2023

Gayan Pathirana[1,2], Kyung Min Noh[1,3*], Dong-Geon Lee[1], Huiji Lee[1] and Jong-Seong Kug[1*]

[1]Division of Environmental Science and Engineering, Pohang University of Science and Technology (POSTECH), Pohang, South Korea.

[2]Department of Oceanography and Marine Geology, FMST, University of Ruhuna, Matara, Sri Lanka.

[3]Department of Atmospheric Sciences, Yonsei University, Seoul, South Korea.

[*]Corresponding author. Email: jskug@postech.ac.kr, km.noh109@gmail.com

Keywords: Indian Ocean Dipole, Biophysical Interaction, Phytoplankton

Abstract

The Indian Ocean Dipole (IOD) is a prominent mode of climate variability in the tropical Indian Ocean (IO). It exerts a significant influence on biological activities in this region. To elucidate the biological response to the IOD, previous research has introduced the Biological Dipole Mode Index (BDMI). However, the delineation of the region by the BDMI has limitations in capturing IOD-induced chlorophyll variations in the IO. By analyzing observational data and historical simulations from a Coupled Model Intercomparison Project (CMIP) model, this study shows that chlorophyll levels in the IO exhibit a dipole pattern in response to IOD. During the developing and mature phases of the IOD, we observe a substantial decrease in chlorophyll in the south-southwest of India, contrasting with a pronounced increase in the southeast of the IO. This response is attributed to anomalous southeasterly winds induced by IOD, which enhance nutrient upwelling in the southeastern IO and suppress it in the south-southwest of India, resulting in corresponding changes in surface chlorophyll blooms. Based on this finding, we propose a new Biological Dipole Index that more robustly explains the surface chlorophyll response to IOD in the tropical IO. This study highlights the profound influence of IOD on oceanic chlorophyll and underscores the importance of a more comprehensive understanding of the associated biophysical interactions.

Introduction

Marine phytoplankton play a key role in global biogeochemical cycles (Field *et al* 1998), contributing to the marine food web (Richardson and Schoeman 2004) and regulating the global climate and carbon cycle (Murtugudde *et al* 2002, Gregg *et al* 2003). Previous studies have reported that surface chlorophyll-a (hereafter chlorophyll) concentrations are an important indicator of phytoplankton productivity (Field *et al* 1998). The western Indian Ocean (IO) has been found to be one of the most productive regions in the tropical oceans (Lee *et al* 2005), and therefore many studies have conducted to understand the associated dynamics of biophysical interactions (Goes *et al* 2005, Wiggert *et al* 2005). For example, Roxy *et al* (2016) investigated the changes in chlorophyll concentration in the western IO and reported an alarming decline in phytoplankton during summer. Further they showed that the enhanced ocean stratification driven by the rapid warming in the IO is a key factor for the declining chlorophyll in the IO. In addition, the biological productivity exhibits a pronounced seasonal cycle in the IO as a result of monsoon variability, which modulates upwelling, entrainment and convective mixing in the upper ocean (McCreary *et al* 1996, Kone *et al* 2009, Vijith *et al* 2016). On the other hand, the seasonal evolution of surface chlorophyll in the IO has been found to be significantly modulated by tropical climate variability, such as El Nino-Southern Oscillation (ENSO, Behrenfeld*et al* 2006, Wiggert *et al* 2009, Currie *et al* 2013, Racault *et al* 2017) and Indian Ocean Dipole (IOD, Brewin *et al* 2012, Park and Kug 2014). Thus, the chlorophyll in the IO is robustly influenced by the local and remote forcings.

The IOD is a prominent and dynamic climate phenomenon that exerts a profound influence on weather and climate patterns throughout the IO region (Saji *et al* 1999). This interannual air-sea coupled climate mode is characterized by a dipole pattern in sea surface temperature (SST) anomalies between the western and eastern equatorial IO (Saji *et al* 1999). IOD typically manifests in two phases: the positive phase is characterized by warmer SST anomalies in the western IO (10° S-10° N, 50° E-70° E) and cooler SST anomalies in the eastern IO (10° S-0°, 90° E-110° E), and vice versa for the negative phase. These SST anomalies trigger variations in the atmospheric circulation, leading to shifts in the position of the Walker circulation, changes in monsoon patterns and altered precipitation regimes in the affected regions (Saji*et al* 1999, Webster *et al* 1999). Thus, the IOD is a crucial component of the Earth's climate system (Saji and Yamagata 2003), affecting not only regional climate variability, but also having far-reaching effects on weather systems (Chan *et al* 2008), agriculture (Ashok and Saji 2007), ecosystems (Marchant *et al*2006, Park and Kug 2014) and socio-economic conditions (Feng *et al* 2022) in countries bordering the IO.

In addition to the effects on the physical structure of the IO, there are biological consequences of IOD with potential importance for the marine ecosystem, fishery resources and carbon sequestration (Currie*et al* 2013). The IOD-induced changes in the surface circulation can lead to upwelling/downwelling and mixing and regulate the supply of nutrients to the surface causing robust changes in surface chlorophyll in the IO (Sarma 2006, Chen *et al* 2013). However, the relationship between IOD and ocean biogeochemistry is complex and depends on the specific phase of IOD (positive or negative) and their regional effects (Sari *et al* 2020). Therefore, the biological response to IOD has been widely studied (Vinayachandran *et al*2002, Chen *et al* 2013, Currie *et al* 2013, Sankar *et al* 2019, Thushara and Vinayachandran 2020, Shi and Wang 2021). For example, Murtugudde *et al* (1999) reported a strong phytoplankton bloom in the eastern equatorial IO, an area characterized by low climatological productivity, due to the intense positive IOD of 1997. Consistently, similar responses were also observed during the 2019 positive IOD event (Shi and Wang 2021). Although similar blooms were observed during the 2006 event, Wiggert *et al* (2009) showed that the biological responses to the 1997 event were more intense, suggesting that IOD intensity is an important factor for the intensity of chlorophyll. Furthermore, Wiggert *et al* (2009) showed that the 1997 and 2006 events caused a decrease in surface chlorophyll in the Arabian Sea (AS), an area characterized by high climatological productivity. On the other hand, several studies have reported an increase in surface chlorophyll in the southeastern AS during negative IOD events due to enhanced Ekman suction and coastal upwelling, as well as a shoaling thermocline in the region (e.g., Thushara and Vinayachandran 2020). Thus, in addition to the differences in chlorophyll intensity, the biological responses to IOD also show a diverse spatial structure.

Given that IOD influences the chlorophyll variability of the tropical IO, Shi and Wang (2021) proposed a biological IOD, and later the authors introduced the biological dipole mode index (BDMI, Shi and Wang 2022) to characterize and quantify IOD-induced changes in surface chlorophyll in the IO. The BDMI is defined as the difference between the average chlorophyll anomaly in the western IO (10° S-10° N, 50° E-70° E) and the eastern IO (10° S-0°, 90° E-110° E), where the chosen region is the same as that used to define the dipole mode index (DMI). However, there are some limitations in the index region that prevent an accurate representation of the chlorophyll variability in response to IOD in the IO. As shown in the composite analysis of positive and negative IODs (Fig. S1), IOD-induced changes in chlorophyll remain weak in the western equatorial IO. This raises questions about the accuracy of using chlorophyll in the western equatorial IO to define the BDMI in previous studies, and therefore possible clarifications are sought to understand the IOD-induced chlorophyll changes (e.g., intensity and spatial pattern) in the tropical IO. Furthermore, understanding these interactions is crucial for understanding the broader ecological and environmental consequences of IOD events over the Indian Ocean. Therefore, in the present study we investigate the biological consequences of IOD.

Data and methods

To investigate the effect of IOD on chlorophyll, we used monthly chlorophyll from the European Space Agency Ocean Color Climate Change Initiative (ESA-OC-CCI v4, Sathyendranath *et al* 2018). In addition, we used monthly SST data from extended reconstructed SST (ERSSTv5, Boyin *et al* 2017), 10 m zonal and meridional winds from National Centers for Environmental Prediction (NCEP2), subsurface temperature from NCEP Global Ocean Data Assimilation System (GODAS, Kanamitsu *et al* 2002), and surface wind stress from European Center for Medium-Range Weather Forecasts (ECMWF) reanalysis (ERA5).

Along with observations, we used historical simulations from 13 CMIP6 coupled general circulation models, including chlorophyll, SST, low-level (850 hPa) winds, subsurface temperature, and nutrients (nitrate and phosphate, Table S1), to provide supporting evidence for the observed relationships. It should be mentioned that these 13 models (Table S1) among CMIP6 models are selected because they only provide full 3-D datasets of ocean biogeochemistry. However, many of the CMIP models fail to reproduce the spatial pattern of climatology in chlorophyll concentrations and interannual variability in the IO (Roxy *et al* 2016). Therefore, following Roxy *et al* (2016), we selected a single model to investigate the biophysical response to IOD based on the pattern correlation coefficient (PCC > 0.5) of mean chlorophyll and the interannual variability of chlorophyll (standard deviation) (Fig. S2). The model chosen is the Geophysical Fluid Dynamics Laboratory Earth System Model (GFDL-ESM4, Dunne *et al* 2020). GFDL-ESM4 simulates the mean climatology of chlorophyll concentrations and the interannual variability of chlorophyll with a relatively small bias compared to the other 12 CMIP6 models (Fig. S2).

In addition, the dipole mode index (DMI) is calculated as the difference between the averaged SST anomaly in the western Indian Ocean (10° S-10° N, 50° E-70° E) and the eastern Indian Ocean (10° S-0°, 90° E-110° E, Saji *et al* 1999). We also examined the biological dipole mode index (BDMI) introduced by Shi and Wang (2022). The BDMI is defined as the difference of average chlorophyll anomaly in the western Indian Ocean (10° S-10° N, 50° E-70° E) and the eastern Indian Ocean (10° S-0°, 90° E-110° E). Here, all anomalies are calculated by removing the seasonal cycle and the long-term linear trend. The datasets have been analyzed for the period 1997-2020 for the observations and for the period 1850-2014 for the CMIP6 simulations.

Results

3.1. Dipole pattern in surface chlorophyll

First, we examined the IOD-induced changes in surface temperature, circulation, and chlorophyll in the tropical IO during the boreal summer to autumn, and the results are shown in Fig. 1. It can be clearly seen that the southeastern IO is cooler and western IO is warmer, and the southeasterly winds are intensified in response to IOD in the observations (Fig. 1a). Consistently, GFDL-ESM4 also shows similar responses, suggesting its ability to reproduce the air-sea interactions in the IO (Fig. 1b). To investigate the influence of IOD on surface chlorophyll changes, we examined the regression patterns of chlorophyll in the tropical IO. The chlorophyll anomalies in the southeastern IO, west of Sumatra, are positively enhanced in response to positive IOD, and vice versa for negative IOD (Fig. 1c). Thus, consistent with previous studies (Currie *et al* 2013, Shi and Wang 2021), high chlorophyll blooms are evident in the southeastern IO during positive IOD events. However, the chlorophyll response in the western equatorial IO remains weaker, raising questions about the accuracy of using chlorophyll in the western equatorial IO to define the BDMI in previous studies. On the other hand, the changes in chlorophyll in the south-southwest coastal region of Indian subcontinent are strong and significant, implying that this region has a more dominant response to IOD than the western equatorial IO. Thus, the strong zonal contrasts of chlorophyll responses exist between the southeastern IO and south-southwest coastal region of Indian subcontinent, indicating a biological dipole in the IO in response to IOD. Despite some changes in the Bay of Bengal and Arabian Sea regions, GFDL-ESM4 also shows consistent results with observations (Fig. 1d). Thus, both composites (Fig. S1) and regression patterns (Fig. 1c) show the emergence of a biological dipole in the tropical IO in response to IOD during the boreal summer to autumn.

To further elucidate the characteristics of the biological dipole, we next examine the correlations between

DMI and surface chlorophyll anomalies. Since previous studies showed that the effect of IOD on chlorophyll is strongest in late boreal summer and autumn (Thushara and Vinayachandran 2020, Shi and Wang 2021), we examined the relationship from August to November. Consistent with the regression patterns (Fig. 1c), the correlation shows more distinctive dipole pattern between the regions of southeastern IO and south-southwest of Indian subcontinent (Fig. 2a). In addition, the correlation remains weaker in the western equatorial IO region, but it is dominant for the chlorophyll response in the south-southwest of Indian subcontinent. Therefore, although there is a dipole pattern in the biological response to IOD, the regions used to explain the BDMI in previous studies might to be less straightforward to represent the chlorophyll responses to the IOD.

Hence, to clearly represent the IOD-induced biological dipole, we select two regions based on the regression (Fig. 1c) and correlation (Fig. 2a) patterns. As shown in Fig. 2b, the strongest chlorophyll response is observed in the regions of Southwest of Indian subcontinent (SWI, 4° N-16° N, 70° E-79° E) and West of Sumatra (WS, 10° S-2° S, 95° E-105° E). Further, to show the dipole-like response of chlorophyll, we examine the correlation between the SWI (WS) chlorophyll index and chlorophyll anomalies in the tropical IO, and the results are shown in Fig. 2b (Fig. 2c). The results clearly show that when chlorophyll anomalies are positively increasing in the SWI (WS) region, chlorophyll anomalies are decreasing simultaneously in the WS (SWI) region. Thus, our results clearly show a dipole pattern in surface chlorophyll in the tropical IO in response to IOD during late summer to autumn. This spatial pattern of correlation has been well captured in GFDL-ESM4 consistent with the observations (Fig. S3). Therefore, we suggest an improved biological dipole index (BDI) as the difference between the average chlorophyll anomaly in the SWI and the WS regions. To show further evidence for the biological dipole, we have also examined the correlation between chlorophyll anomalies of the SWI and WS regions and found a significant negative relationship (Fig. S4). It is worth noting that the correlation during June to November is –0.43, and the correlation becomes stronger (–0.48 for the observations, and –0.53 for the GFDL-ESM4) during August to October, implying that the dipole pattern in chlorophyll is more dominant during late summer to autumn.

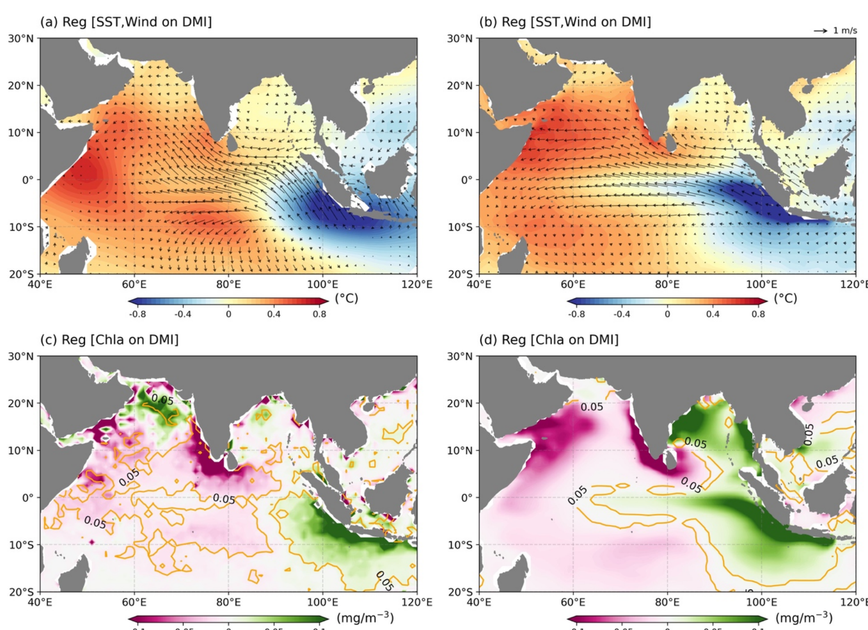

Figure 1. Regressed SST (color shading) and 850 hPa winds (vector) on DMI for (a) observations during 1997-2020 and (b) CMIP6 model during 1850-2014. Regressed surface chlorophyll (color shading) on DMI for (c) observations and (d) CMIP6 model. In (a) and (b) only significant values at the 95% confidence interval are displayed. Significant regions at the 95% confidence interval are marked by contours in (c) and

(d). The chosen season is boreal summer to autumn (June to November).

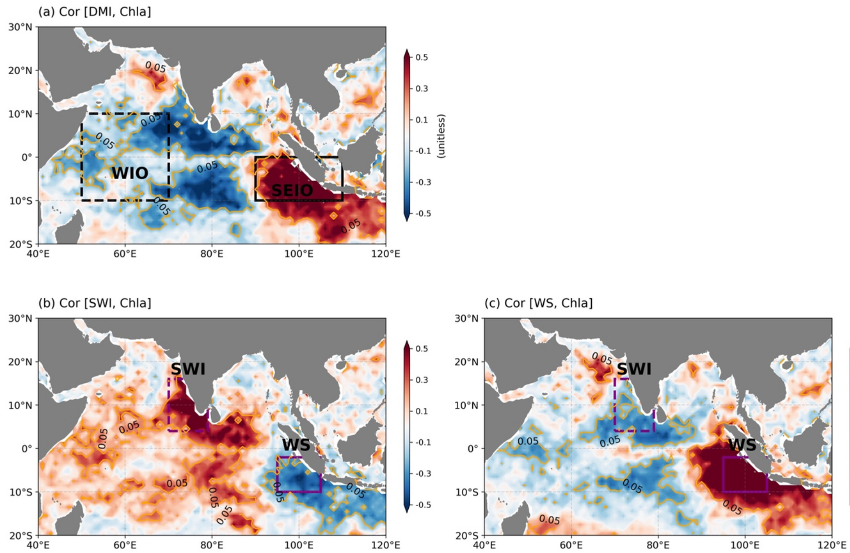

Figure 2. (a) Correlation between DMI and surface chlorophyll anomalies. The black solid and dashed square indicates the southeastern IO (SEIO) and western IO (WIO) region respectively, used to define the DMI. (b) Correlation between SWI chlorophyll index and surface chlorophyll anomalies, and (c) correlation between WS chlorophyll index and surface chlorophyll anomalies. In (b) and (c) the purple solid and dashed square indicates the SWI and WS regions used to define the biological dipole index (BDI). In each plot significant regions at the 95% confidence interval are marked by contours.

To explore the characteristics of IOD and BDI, we further examined the amplitude and phase locking (Fig. 3). As shown in Fig. 3, both in the observations and GFDL-ESM4, IOD and BDI show a dominant seasonal dependency with a peak phase in autumn. In addition, consistent with previous studies IOD peaks in October in the observations (Li *et al* 2003, Saji *et al* 1999), while the BDI shows an early peak (September, Fig. 3a). On the other hand, although the BDI peak month in GFDL-ESM4 is consistent with observations, IOD in the GFDL-ESM4 shows an early peak compared to the observations (Fig. 3c). However, apart from the differences in the peak month, both observations and model show the strong phase locking of IOD and BDI in the boreal autumn.

We further examined the relationship between BDI and IOD during September to October (Fig. 3b). The months of September and October have been chosen as the peak months of the two indices. The results clearly show that there is a strong and significant correlation between BDI and IOD amplitudes during autumn. In agreement with the observations, GFDL-ESM4 also shows a strong and significant correlation (-0.85, Fig. 3d). We also examined the correlation between BDMI (defined according to Shi and Wang 2022) and IOD during autumn and found that the correlation ($r = -0.62$) is lower compared to that of BDI (Fig. S5). Also, the previous BDMI does not capture chlorophyll variability during extreme events because the region used to define the index does not reflect well the changes in chlorophyll in response to IOD. For example, the extreme negative IOD in 2016 is not apparent in the BDMI (BDMI=0.01 for September 2016, Fig. S5), but the event is well represented in the BDI (BDI=0.86 for September 2016, Fig. 3c). Therefore, compared to the BDMI in previous studies, the BDI can well represent the IOD-induced responses in chlorophyll. Thus, we demonstrate the presence of the biological dipole pattern in the tropical IO and propose a new definition (BDI) that can actively capture the variability of chlorophyll in response to IOD.

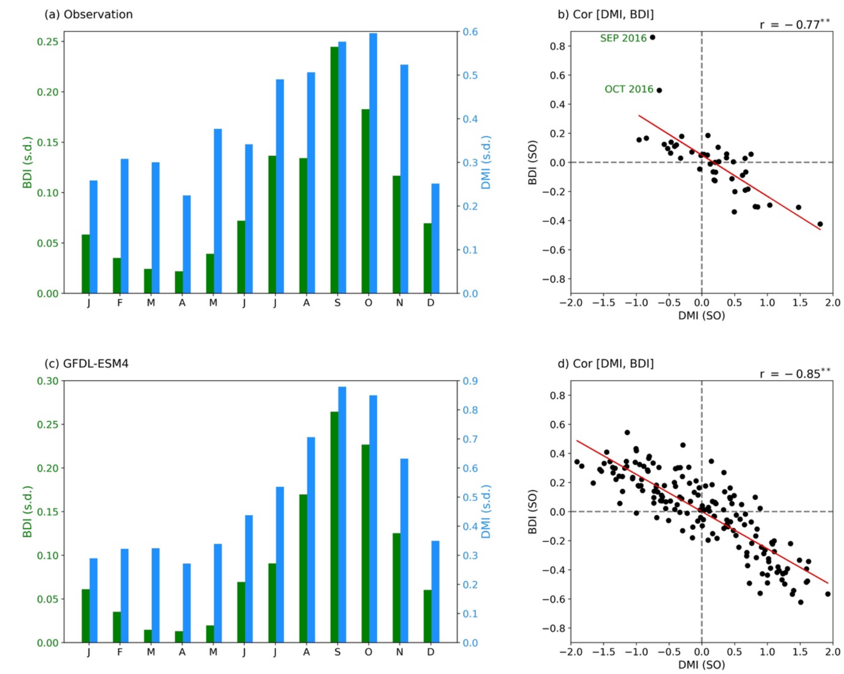

Figure 3. Observed interannual variability of (a) DMI (blue) and BDI (green) during 1997-2020 and observed (b) correlation between DMI and BDI during 1997-2020 for September to October. (c) and (d), same as (a) and (b), respectively, but for GFDL-ESM4 model during 1850-2014. The regressed line is shown in red, and the correlation (r) shown in the plot is significant at the 99% confidence level. In (b), September and October months of 2016 extreme negative IOD event are marked using green labels.

3.2. How does IOD produce dipole variability of the chlorophyll in the Indian Ocean?

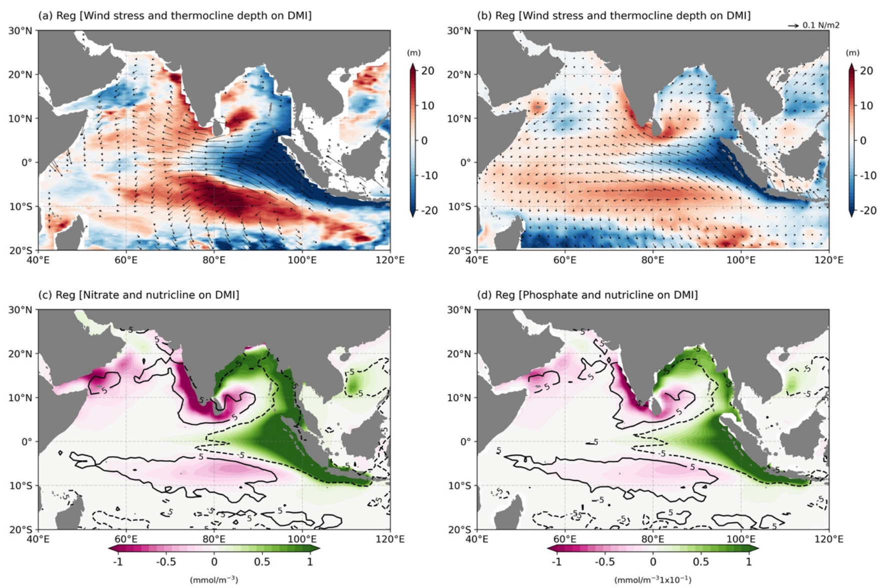

Figure 4. Regressed thermocline (color shading) and surface wind stress (vector) on DMI for (a) observations and (b) GFDL-ESM4 model. For thermocline and wind stress only significant regions at the 95% confidence interval are displayed. Regressed upper 50m (c) Nitrate and (d) Phosphate on GFDL-ESM4 model. For nutrients, significant regions at the 95% confidence interval are displayed. The contour lines indicate the regressed nutricline (m) on DMI. Here, thermocline and nutricline are defined as the depth of the maximum vertical gradient of potential temperature and nutrients, respectively.

To understand how IOD modulates surface chlorophyll in the tropical IO, we next examine IOD-induced changes in atmosphere-ocean coupled systems (e.g., surface wind stress, thermocline, and nutrients such as nitrate and phosphate, Fig. 4). As shown in Fig. 4a, southeasterly wind stress is significantly enhanced in response to IOD in the eastern equatorial IO. Given the importance of strong air-sea coupling in this region (Bjerknes feedback; Bjerknes 1969), IOD-induced southeasterly winds are favorable for thermocline shoaling in the eastern equatorial IO (Fig. 4a). This results in cooler SSTs (Fig. 1a), indicating strong upwelling in the southeastern IO, west of Sumatra. On the other hand, the wind stress and thermocline response in the western equatorial IO remains weaker, suggesting that IOD-induced upwelling/downwelling in this region is weaker or even negligible during late summer to autumn. Interestingly, consistent with the chlorophyll response (Fig. 1c), the southwest region of Indian subcontinent has stronger southeasterly winds and a deeper thermocline, suggesting that the IOD-induced upwelling/downwelling is stronger in this region compared to the western equatorial IO. Thus, upwelling (downwelling) is enhanced in the WS (SWI) in response to IOD. The IOD-induced changes in surface wind stress and thermocline in GFDL-ESM4 are consistent with the observations (Fig. 4b).

In general, nutrients such as nitrate and phosphate are essential for phytoplankton blooms in the tropical IO (i.e., Roxy *et al* 2016). To further illustrate the variability in nutrient supply to the surface in response to IOD, we have examined the regression patterns of nitrate (Fig. 4c), phosphate and nutricline (Fig. 4d). The nutricline is defined as the depth of the maximum vertical gradient of each nutrient. Consistent with the changes in the thermocline, the results clearly show an increase in nutrients in the eastern equatorial IO and a decrease in the south-southwestern region of India. Thus, IOD-induced changes in the upwelling/downwelling process are a key factor in chlorophyll variability, leading to a biological dipole in response to IOD in the tropical IO.

Discussion

Marine primary productivity in the IO is highly sensitive to the ocean-atmosphere dynamics associated with the IOD (Currie *et al*2013, Wiggert *et al* 2009), and it is therefore essential to understand the profound effect of the IOD on oceanic chlorophyll. Previous studies (Shi and Wang 2021, 2022) have attempted to explain the biological response of IOD using BDMI. However, there are discrepancies between physical response and biological response in the index region that prevent an accurate representation of the IOD-induced chlorophyll variability. As can be seen from the composites of positive and negative IODs, the change in the western equatorial IO is negligible. Thus, despite the dipole pattern in the biological response to IOD, the regions used to explain the BDMI in previous studies have limitations to express the actual biological variability in the IO. On the other hand, even if there is a biological dipole response, the BDMI is not able to capture the chlorophyll variability well. For example, the BDMI does not well reflect the extreme events (i.e., 2016 negative IOD, Fig. 3b and Fig. S5). Therefore, it suggests the need for an accurate index that can deeply explain the IOD-induced chlorophyll variability in the tropical IO.

Furthermore, we found discrepancies between observations and CMIP6 models. Although GFDL-ESM4 is closer to the observations, the remaining 12 models do not well capture the climatology and interannual variability of chlorophyll in the tropical IO, suggesting biases in current biogeochemical models (Roxy *et al* 2016, Lim *et al*2018). In addition, we have not used observed nutrients to quantify IOD-induced changes, so it will be important to construct advanced observational systems to understand the associated biophysical interactions in detail. Nevertheless, the observations and the model used in our study provide sufficient evidence for a general understanding of the IOD-induced changes in marine phytoplankton in the tropical IO.

As marine phytoplankton play a key role in the marine food web, environment, and global climate, understanding their changes in response to tropical climate variability has important implications. Studies have shown that IOD-induced changes in upwelling/downwelling and surface chlorophyll concentrations (an indicator of biological productivity) are likely to affect the abundance of economically valuable tuna stocks, catch rates, fishing grounds and other pelagic fish species in the IO (Wiggert *et al* 2009, Lan *et al* 2013, Gaol *et al*2015, Setyohadi *et al* 2021, Wang *et al* 2023). Therefore, changes in phytoplankton blooms can modulate fisheries production and ecosystem functions, and also can cause major environmental problems (Dai *et al* 2023). Thus, understanding IOD-induced changes in marine phytoplankton has direct and important implications for fisheries and environmental management in the IO.

Conclusion

We have investigated the IOD-induced surface chlorophyll responses in the IO using both observations and a CMIP6 earth system model, and show the strong zonal contrast of chlorophyll blooms between the southeastern IO and the south-southwestern region of the Indian subcontinent. This strong zonal contrast indicates a biological dipole in the IO in response to IOD. Furthermore, we show that the IOD-induced changes in the nutrient upwelling/downwelling process are a key factor in the chlorophyll variability leading to the biological dipole in the tropical IO. Finally, since the previously defined BDMI has limitations in representing the IOD-induced chlorophyll variability, we propose a new biological dipole index (BDI) that can robustly explain surface chlorophyll changes in the tropical IO in response to IOD. In addition, we highlight the need for a better understanding of the associated biophysical interactions in the tropical IO.

Acknowledgements

We thank the World Climate Research Programme and the climate modelling groups for coordinating, producing, and providing the CMIP6 data. All graphs and analyses were performed using Python v. 3.9 and supportive packages. This work was supported by the National Research Foundation of Korea (NRF-2018R1A5A1024958).

Data Availability Statement

The CMIP6 data used in this study is available at https://esgf-node.llnl.gov/projects/cmip6/. ERSST data is available at https://psl.noaa.gov/data/gridded/data.noaa.ersst.v5.html. Chlorophyll data is available at https://www.oceancolour.org. NCEP data is available at https://psl.noaa.gov/data/. ERA5 data is available at https://cds.climate.copernicus.eu/.

Ethical statement

Not applicable

ORCID iDs

Gayan Pathirana – https://orcid.org/0000-0002-4670-579X

Kyung Min Noh – https://orcid.org/0000-0003-4233-4490

Jong-Seong Kug – https://orcid.org/0000-0003-2251-2579

References

Ashok K and Saji N H 2007 On the impacts of ENSO and Indian Ocean dipole events on sub-regional Indian summer monsoon rainfall *Nat. Hazards* **42** 273–285

Behrenfeld M *et al* 2006 Climate-driven trends in contemporary ocean productivity. *Nature* **444** 752–755

Bjerknes J 1969 Atmospheric teleconnections from the equatorial Pacific*Mon. Wea. Rev.* **97** 163–172

Boyin H *et al* 2017 NOAA Extended Reconstructed Sea Surface Temperature (ERSST), Version 5 NOAA National Centers for Environmental Information

Brewin R J W *et al* 2012 The influence of the Indian Ocean Dipole on interannual variations in phytoplankton size structure as revealed by Earth Observation *Deep Sea Res. Part II* **77**–**80** 117–127

Chan S C, Behera S K and Yamagata T 2008 Indian Ocean Dipole influence on south American rainfall *Geophysical Research Letters***35** (14) L14S12

Chen X *et al* 2013 Episodic phytoplankton bloom events in the Bay of Bengal triggered by multiple forcings *Deep Sea Research I***73** 17–30

Currie J C *et al* 2013 Indian Ocean Dipole and El Niño/Southern Oscillation impacts on regional chlorophyll anomalies in the Indian Ocean *Biogeosciences* **10** 6677–6698

Dai Y *et al* 2023 Coastal phytoplankton blooms expand and intensify in the 21st century *Nature* **615** 280–284

Dunne J P *et al* 2020 The GFDL Earth System Model Version 4.1 (GFDL-ESM 4.1): Overall Coupled Model Description and Simulation Characteristics *Journal of Advances in Modeling Earth Systems***12** (11) e2019MS002015

Feng P *et al* 2022 Increasing dominance of Indian Ocean variability impacts Australian wheat yields *Nat. Food* **3**862–870

Field C B, Behrenfeld M J, Randerson J T and Falkowski P 1998 Primary production of the biosphere: Integrating terrestrial and oceanic components *Science* **281** (5374) 237

Gaol L R *et al* 2015 Variability of satellite-derived sea surface height anomaly, and its relationship with Bigeye tuna (*Thunnus obesus*) catch in the Eastern Indian Ocean *European Journal of Remote Sensing* **48** (1) 465-477

Goes J I, Thoppil P G, Gomes H R and Fasullo J T 2005 Warming of the Eurasian landmass is making the Arabian Sea more productive*Science* **308** (5721) 545–547

Gregg W W *et al* 2003 Ocean Primary Production and Climate: Global Decadal Changes *Geophys. Res. Lett.* **30** (15) 10–13

Kanamitsu M *et al* 2002 NCEP-DOE AMIP-II Reanalysis (R-2)*Bulletin of the American Meteorological Society* 1631-1643

Kone V, Aumont O, Levy M and Resplandy L 2009 Physical and biogeochemical controls of the phytoplankton seasonal cycle in the Indian Ocean: A modeling study *Geophysical Monograph Series* **185** 147–166

Lan K W, Evans K and Lee M A 2013 Effects of climate variability on the distribution and fishing conditions of yellowfin tuna (*Thunnus albacares*) in the western Indian Ocean *Climatic Change* **119** 63–77

Lee P -F, Chen I -C and Tzeng W -N 2005 Spatial and temporal distribution patterns of bigeye tuna (*Thunnus obesus*) in the Indian Ocean *Zool. Stud. Taipei* **44** (2) 260

Li T, Wang B, Chang C P and Zhang Y 2003 A theory for the Indian Ocean dipole–zonal mode *Journal of Atmospheric Sciences* **60** (17) 2119– 2135

Lim H G, Park J Y and Kug J -S 2018 Impact of chlorophyll bias on the tropical Pacific mean climate in an earth system model *Clim. Dyn.* **51** 2681–2694

Marchant R, Mumbi C, Behera S and Yamagata T 2007 The Indian Ocean dipole–the unsung driver of climatic variability in East Africa *Afr. J. Ecol.* **45** 4–16

McCreary J P, Kohler K E, Hood R R and Olson D B 1996 A four-component ecosystem model of biological activity in the Arabian Sea *Progress in Oceanography* **37** (3–4) 193–240

Murtugudde R *et al* 1999 Ocean color variability of the tropical Indo-Pacific basin observed by SeaWiFS during 1997–1998 *J. Geophys. Res.* **104** (18) 351–366

Murtugudde R *et al* 2002 Effects of penetrative radiation on the upper tropical ocean circulation, *J. Clim.* **15** (5) 470–486

Park J Y and Kug J -S 2014 Marine biological feedback associated with Indian Ocean Dipole in a coupled ocean/biogeochemical model. *Clim. Dyn.* **42** 329–343

Racault M F *et al* 2017 Impact of El Nino Variability on Oceanic Phytoplankton *Frontiers in Marine Science* **4**

Richardson A J and Schoeman D S 2004 Climate Impact on Plankton Ecosystems in the Northeast Atlantic *Science* 305(5690) 1609–1612

Saji N H and Yamagata T 2003 Possible impacts of Indian Ocean Dipole mode events on global climate *Clim. Res.* **25** 151–169

Saji N H, Goswami B N, Vinayachandran P N and Yamagata T 1999 A dipole mode in the tropical Indian Ocean *Nature* **401** 360–363

Sankar S *et al* 2019 The influence of tropical Indian Ocean warming and Indian Ocean Dipole on the surface chlorophyll concentration in the eastern Arabian Sea *Biogeosciences Discussion*

Sari Q W *et al* 2020 Surface chlorophyll-*a* variations in the Southeastern Tropical Indian Ocean during various types of the positive Indian Ocean Dipole events *Int. J. Remote Sens.* **41** 171–184

Sarma V V S S 2006 The influence of Indian Ocean Dipole (IOD) on biogeochemistry of carbon in the Arabian Sea during 1997–1998 *Journal of Earth System Science* **115** (4) 433–450

Sathyendranath S *et al* 2018 ESA ocean colour climate change initiative (Ocean_Colour_cci): Global remote sensing reflectance gridded on a sinusoidal projection, version 3.1. Data, *Centre for Environmental Data Analysis* 04 July 2018 https://doi.org/10.5285/9c334fbe6d424a708cf3

Setyohadi D, Zakiyah U, Sambah A B and Wijaya A 2021 Upwelling Impact on *Sardinella lemuru* during the Indian Ocean Dipole in the Bali Strait Indonesia *Fishes* 6(1) 8

Shi W and Wang M 2021 A biological Indian Ocean Dipole event in 2019 *Sci. Rep.* **11** 2452

Shi W and Wang M 2022 Biological dipole mode indices: New parameters to characterize the physical and biological processes of the Indian Ocean Dipole event *Progress in Oceanography* 102847

Thushara V and Vinayachandran P N 2020 Unprecedented surface chlorophyll blooms in the southeastern Arabian Sea during an extreme negative Indian Ocean Dipole *Geophysical Research Letters* **47** (13) e2019GL085026

Vijith V, Vinayachandran P N, Thushara V, Amol P, Shankar D and Anil A C 2016 Consequences of inhibition of mixed-layer deepening by the West India Coastal Current for winter phytoplankton bloom in the northeastern Arabian Sea *Journal of Geophysical Research: Oceans* **121**6583–6603

Vinayachandran P N, Murthy V S N and Babu V R 2002 Observations of barrier layer formation in the Bay of Bengal during summer monsoon.*Journal of Geophysical Research* **107** (C12) 8018

Wang Y, Zhang F, Geng Z, Zhang Y, Zhu J and Dai X 2023 Effects of Climate Variability on Two Commercial Tuna Species Abundance in the Indian Ocean *Fishes* **8** (2) 99

Webster P J, Moore A M, Loschnigg J P and Leben R R 1999 Coupled ocean-atmosphere dynamics in the Indian Ocean during 1997–98*Nature* **401** 356–360

Wiggert J D, Vialard J and Behrenfeld M J 2009 Basin-wide modification of dynamical and biogeochemical processes by the positive phase of the Indian Ocean Dipole during the SeaWiFS era *Indian Ocean Biogeochemical Processes and Ecological Variability* **185**385–407

Wiggert J, Hood R, Banse K and Kindle J 2005 Monsoon-driven biogeochemical processes in the Arabian Sea *Prog. Oceanogr.***65** (2–4) 176–213